

Magnetic properties of the ordered and disordered double perovskite $\text{Sr}_2\text{Fe}_{1+x}\text{Mo}_{1-x}\text{O}_6$ ($-1 \leq x \leq 1/3$)

J.R. Suárez^{1,a}, F. Estrada^{2,3}, O. Navarro², and M. Avignon¹

¹ Institut Néel, CNRS and Université Joseph Fourier - BP 166, 38042 Grenoble Cedex 9, France

² Instituto de Investigaciones en Materiales, Universidad Nacional Autónoma de México - Apartado Postal 70-360, 04510 México D. F., México

³ Centro de Investigación en Materiales Avanzados, S. C., Miguel de Cervantes 120, Complejo Industrial Chihuahua, 31109 Chihuahua Chih., México

Received 7 August 2011 / Received in final form 27 September 2011

Published online 3 November 2011 – © EDP Sciences, Società Italiana di Fisica, Springer-Verlag 2011

Abstract. We have studied the effect of cationic disorder on the spin polarization of the double perovskite system $\text{Sr}_2\text{Fe}_{1+x}\text{Mo}_{1-x}\text{O}_6$ with $-1 \leq x \leq 1/3$. The composition $x = 0$ corresponds to the well-known double-perovskite $\text{Sr}_2\text{FeMoO}_6$, which is expected to have complete spin polarization, however all samples present some degree of Fe/Mo disorder which reduces the tunneling magnetoresistance in granular samples. We consider an electronic model within the renormalized perturbation expansion Green's functions, consisting in a correlated electron picture with localized Fe-ions and itinerant electrons interacting with the local spins via a double-exchange type mechanism. Our results show the influence of disorder on the density of states and the ground-state properties, particularly on the spin polarization over the whole range of x .

1 Introduction

Transition metal oxides have been widely investigated in view of their attractive properties for potential spintronic applications [1]. In particular, half-metallic ferromagnetic oxides have been searched as a source of spin polarized currents. Additionally, its large magnetoresistance (MR) could be used in information storage devices. The double perovskite $\text{Sr}_2\text{FeMoO}_6$ (SFMO) is a ferromagnetic half-metal with a high Curie temperature $T_C \sim 400$ K and substantial low-field MR [2]. Its enhanced T_C , complete spin polarization at the Fermi level and substantially larger low-field MR as compared to manganites, generate a great interest in view of its possible magnetoelectronic applications.

The ordered structure of SFMO consists of corner-sharing BO_6 octahedra with $\text{B} = \text{Fe}, \text{Mo}$ alternating along the three crystallographic axes of the perovskite structure, while Sr lies on the dodecahedral sites. The Fe/Mo positions denoted Fe (S) and Mo (S) can be viewed as a two interpenetrated BO_6 face-centered cubic sublattices. In the fully ordered structure, ferromagnetism and half-metallicity in SFMO have been explained [3] making use of a strongly correlated picture, consisting of $\text{Fe}^{3+}(3d^5)$ localized ions in a high-spin $S = 5/2$ configuration, together with Mo^{6+} cores and one itinerant electron per formula unit (f.u.), which can hop to Fe sites only with

an antiparallel orientation to the localized spin, stabilizing a ferromagnetic arrangement of local spins and fully opposite spin-polarized itinerant electrons. This view is consistent with ab initio calculations [2,4,5]. Accordingly, the saturation magnetization per f.u. is $M_S = 4\mu_B$, however, the measured value in normal prepared samples results to be invariably lower [2,6,7]. Additionally, a spin polarization $P \approx 0.85$ has been measured [8] in a SFMO-based tunnel junction device instead of the full polarization value $P = 1$ reached with the saturation magnetization. This deviation of the theoretical values is attributed to some degree of cationic disorder present in the samples, in which Fe and Mo interchange their crystallographic positions, creating the so-called anti-sites (AS). Magnetoresistive properties of SFMO are connected to the amount of the cationic ordering [8–10].

In view of the difficulty to have a full control of the disordering process, the off-stoichiometric system $\text{Sr}_2\text{Fe}_{1+x}\text{Mo}_{1-x}\text{O}_6$ ($-1 \leq x \leq 0.25$) has been proposed to elucidate how the presence of AS defects modifies the magnetic properties as compared to the ideal $x = 0$ composition [11]. The simple idea is to control atomic arrangements resulting from disorder by controlling the composition x . For $x = 0$, disorder generates both Fe (S)–O–Fe (AS) and Mo (S)–O–Mo (AS) nearest-neighbors (n.n) pairs which are the key in determining the electronic and magnetic properties. The Mo (S)–O–Mo (AS) bonds open new hopping channels available for both spin directions, thereby depolarizing the conduction

^a e-mail: jaimeunam@gmail.com

band [12,13]. In the Mo-rich regime ($x < 0$), such Mo (S)–O–Mo (AS) bonds are favored even in the ordered situation, although Fe (S)–O–Fe (AS) bonds are also present due to disorder. On the other hand, in the Fe-rich side ($x > 0$), the excess of Fe ions replacing Mo inevitably produces n.n Fe (S)–O–Fe (AS) pairs. The saturation magnetization M_S shows the remarkable behavior of first increasing with x up to $x = 0$ for $x < 0$ and then decreasing for $x > 0$ [11], which can be qualitatively understood in terms of Fe local spins. Basically, for $x \leq 0$, M_S increases with x primarily because the number of local spins increases in a ferromagnetic background while the decrease in the regime $x \geq 0$ can be explained only considering that n.n Fe (S) and Fe (AS) local spins are antiferromagnetically coupled [11]. The electronic structure of ordered $\text{Sr}_2\text{Fe}_{1+x}\text{Mo}_{1-x}\text{O}_6$ has been studied [14] using first-principles density functional theory DFT+U with an effective on-site correlation energy only on Fe sites, though it has been shown [13] that electronic interaction on Mo sites is also important in determining an appropriate electronic model with disorder. In this paper we propose a correlated picture on Fe and Mo sites to investigate the effect of disorder on the electronic and magnetic properties of the system over the whole range $-1 \leq x \leq 1/3$. We will show that the presence of AS, either by cationic disorder and/or excess or deficiency of Fe/Mo in the structure, is detrimental to the half-metallic character of the system. Our results are compared with experimental data showing a good agreement.

2 Model

Cationic disorder is present in all SFMO samples, but how AS are distributed through the system is not evident. Different local environments and/or antiphase domains, in which short-range order exists even in samples with a high degree of long-range disorder, have been suggested [15,16]. Complexity is added considering the off-stoichiometric system in which the Fe/Mo proportion is not preserved. In view of the nanosized characteristics of the domains evidenced in the stoichiometric compounds [16], in this paper we assume an uncorrelated distribution of AS defects in $\text{Sr}_2\text{Fe}_{1+x}\text{Mo}_{1-x}\text{O}_6$ ($-1 \leq x \leq 1/3$) defining the order parameter a ($1/2 \leq a \leq 1$) as the probability to find Fe and Mo in their correct positions, respectively sublattices α and β of the ordered structure. In the Fe rich regime ($x \geq 0$), we have the proportions $p_{\text{Mo}}^\beta = a(1-x)$, $p_{\text{Fe}}^\beta = 1-a(1-x)$, $p_{\text{Fe}}^\alpha = x+a(1-x)$ and $p_{\text{Mo}}^\alpha = (1-a)(1-x)$. Similarly, in the Fe deficient regime ($x \leq 0$), we have $p_{\text{Fe}}^\alpha = a(1+x)$, $p_{\text{Mo}}^\alpha = 1-a(1+x)$, $p_{\text{Fe}}^\beta = (1-a)(1+x)$ and $p_{\text{Mo}}^\beta = a(1+x)-x$. Preliminary calculations, in the stoichiometric case, including short-range order show that this does not modify qualitatively the present picture.

Following Carvajal et al. [3], we consider a strongly correlated description for Fe with the configuration $\text{Fe}^{3+}(3d^5)$ forming high-spin $S = 5/2$ localized spins and $\text{Mo}^{6+}(4d^0)$ cores. Additionally we have $n = 1 - 3x$ nominally Mo

electrons, which are itinerant providing the metallic behavior of the system. Therefore, Fe cannot retain its trivalent state for $x \geq 1/3$, as Mo cannot take a valency larger than 6+. As discussed above, it is clear that Fe (S) and Fe (AS) generated by disorder and/or excess of Fe in the structure are antiferromagnetically ordered [11], so we consider all Fe (S) local spins lying on sublattice α to be $\uparrow (+)$ and $\downarrow (-)$ for Fe (AS) on sublattice β . On the other hand, correlations are weak on Mo sites [17], the end member SrMoO_3 being known as a paramagnetic metal [18], so that Mo (S)–O–Mo (AS) hopping channels are open for both up and down spins.

Furthermore, on-site electronic energies E_{Fe} and E_{Mo} are different from AS energies E'_{Fe} and E'_{Mo} due to different environments. Essentially, in the ideal case an electron on a Fe^{3+} site is surrounded by Mo^{6+} ions and vice versa. Away from this case, electrons on all sites can be surrounded both by Fe^{3+} and Mo^{6+} ions, then under the influence of a less or more attractive potential. Diagonal energies have been estimated by ab initio calculations [12], finding an energy difference $E'_{\text{Fe}} - E_{\text{Fe}} \approx 1$ eV, and a much weaker effect of the environment for Mo, so we will take $E_{\text{Mo}} = E'_{\text{Mo}}$. Making a Madelung-like analysis and taking E_{Fe} as a reference energy, we find that on-site energies for the Fe-rich regime are $E'_{\text{Fe}} = E_{\text{Fe}} + \delta(2a-1)(1-x)$ and $E_{\text{Mo}} = E_{\text{Fe}} + \Delta_0 - \delta[1-a(1-x)]$, and the corresponding relations for the Fe-deficient regime are $E'_{\text{Fe}} = E_{\text{Fe}} + \delta(2a-1)(1+x)$ and $E_{\text{Mo}} = E_{\text{Fe}} + \Delta_0 - \delta(1-a)(1+x)$, with $\Delta_0 = E_{\text{Mo}}^0 - E_{\text{Fe}}^0$ the charge transfer energy in the ideal ordered state. According to band structure calculations [2], bandwidth w corresponding to Fe–Mo hopping is about 1 eV, so a good estimate for δ seems to be $\delta = w$.

The threefold degenerate t_{2g} orbitals give rise to a conduction band described by a tight-binding model. Itinerant electrons can hop between Fe and Mo t_{2g} orbitals by means of O p states with the same symmetry, giving three degenerate two-dimensional bands with coordination $z = 4$ and leading to an intermediate valence configuration, $\text{Fe}^{(3-\zeta)+}$ and $\text{Mo}^{(5+\zeta)+}$, with $0 \leq \zeta \leq 1$. Figure 1 shows a scheme for the local and itinerant spin configurations in the ideal structure and with AS defects. We consider only n.n hoppings i.e. between the two sublattices. In the first case, only one itinerant electron spin channel is open between Fe–Mo because all Fe $3d$, let's say spin up orbitals, are occupied, so itinerant electrons can hop to Fe sites only with spin down orientation, stabilizing a system of spin polarized itinerant electrons moving in a ferromagnetic background. When Fe (AS) and Mo (AS) are present, Fe (AS)–Mo (AS) hopping becomes allowed to spin up itinerant electrons. Note that Fe–Fe hoppings are not allowed due to the antiferromagnetic orientation of local spins.

With the aim of calculate the density of states (DOS) for itinerant electrons we shall obtain the local Green' functions within the renormalized perturbation expansion (RPE) [19]. In an alternating Bethe lattice in the limit $z \rightarrow \infty$ and zt^2 scaled as $w^2/4$, the local average Green's functions take the dynamical mean-field (DMF) form $G_{ii,\sigma}^{-1} = \omega - \varepsilon_i - \sum_{l \neq i} t^2 G_{ll,\sigma}$, where ε_i is

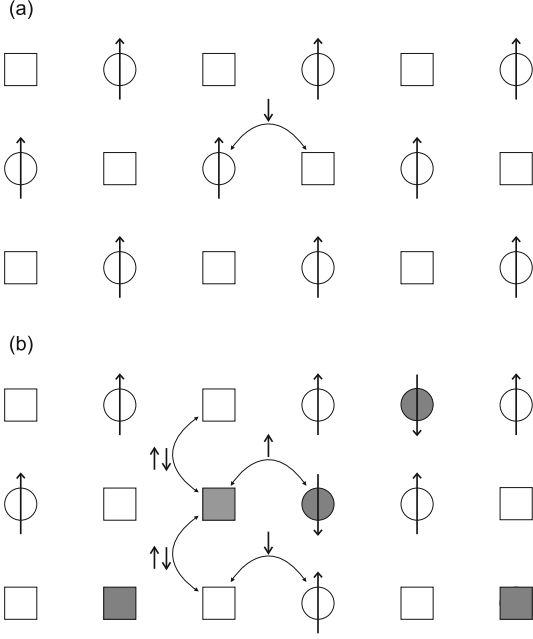


Fig. 1. Scheme of the spin configuration for Fe and Mo ions (a) in a perfect lattice $a = 1$ and $x = 0$ (empty circles and squares respectively) and (b) with AS defects $a \neq 1$ and/or $x \neq 0$ (filled circles and squares respectively). Large (small) arrows indicate the localized (itinerant) spin orientation. Allowed hoppings of itinerant electrons in different environments are also shown.

the corresponding on-site energy and the summation is over all nearest neighbors sites. In the presence of disorder this requires to take an average over the different n.n atomic configurations, thus simply considering the probabilities p_{Fe}^α , p_{Mo}^α , etc defined above. This averaging procedure is an extension similar to the usual coherent potential approximation in the case of random alloys [20]. It includes both the disordering of the site energies and the difference in hopping parameters. The Green's functions for an itinerant electron with spin \downarrow are given by

$$G_{\downarrow+}^{\alpha\text{Fe}} = \frac{1}{\omega - \tilde{E}_{\text{Fe}} - \frac{w^2}{4} p_{\text{Mo}}^\beta G_{\downarrow}^{\beta\text{Mo}}}, \quad (1)$$

$$G_{\downarrow}^{\beta\text{Mo}} = \frac{1}{\omega - \tilde{E}_{\text{Mo},\downarrow} - \frac{w^2}{4} p_{\text{Fe}}^\alpha G_{\downarrow+}^{\alpha\text{Fe}} - \frac{w'^2}{4} p_{\text{Mo}}^\alpha G_{\downarrow}^{\alpha\text{Mo}}}, \quad (2)$$

$$G_{\downarrow}^{\alpha\text{Mo}} = \frac{1}{\omega - \tilde{E}'_{\text{Mo},\downarrow} - \frac{w'^2}{4} p_{\text{Mo}}^\beta G_{\downarrow}^{\beta\text{Mo}}}, \quad (3)$$

while for spin \uparrow ,

$$G_{\uparrow-}^{\beta\text{Fe}} = \frac{1}{\omega - \tilde{E}'_{\text{Fe}} - \frac{w^2}{4} p_{\text{Mo}}^\alpha G_{\uparrow}^{\alpha\text{Mo}}}, \quad (4)$$

$$G_{\uparrow}^{\alpha\text{Mo}} = \frac{1}{\omega - \tilde{E}'_{\text{Mo},\uparrow} - \frac{w^2}{4} p_{\text{Fe}}^\beta G_{\uparrow-}^{\beta\text{Fe}} - \frac{w'^2}{4} p_{\text{Mo}}^\beta G_{\uparrow}^{\beta\text{Mo}}}, \quad (5)$$

$$G_{\uparrow}^{\beta\text{Mo}} = \frac{1}{\omega - \tilde{E}_{\text{Mo},\uparrow} - \frac{w'^2}{4} p_{\text{Mo}}^\alpha G_{\uparrow}^{\alpha\text{Mo}}}, \quad (6)$$

$\mu = \pm$ denotes the Fe local spin orientation in each sublattice. Bandwidths w and w' , for Fe–Mo and Mo–Mo hoppings respectively, are related by $w' = qw$ with $q > 1$ because the large extension of the Mo 4d states [21]. The value $q \sim 2$ seems to be compatible with ab initio calculations. As it was pointed before, it is essential to consider electronic correlations both on Fe and Mo ions. \tilde{E}_{Fe} and $\tilde{E}_{\text{Mo},\sigma}$ (\tilde{E}'_{Fe} and $\tilde{E}'_{\text{Mo},\sigma}$) are effective Fe and Mo site (anti-sites) energies including electronic correlations. Fe itinerant electron energies have no spin dependence because it is automatically assigned by the localized spin. The intra-atomic correlations among itinerant electrons are given by

$$H_C^{\text{Mo}} = (U^{\text{Mo}} + 2J^{\text{Mo}}) \sum_{i,\nu} n_{i\nu\uparrow} n_{i\nu\downarrow} + U^{\text{Mo}} \sum_{i,\nu,\nu' \neq \nu} n_{i\nu\uparrow} n_{i\nu'\downarrow} + (U^{\text{Mo}} - J^{\text{Mo}}) \sum_{i,\nu,\nu' \neq \nu,\sigma} n_{i\nu\sigma} n_{i\nu'\sigma}, \quad (7)$$

$$H_C^{\text{Fe}} = (U^{\text{Fe}} - J^{\text{Fe}}) \sum_{j,\nu,\nu' \neq \nu,\sigma} n_{j\nu\sigma} n_{j\nu'\sigma}, \quad (8)$$

ν and ν' label the three degenerated t_{2g} orbitals. On Mo sites both intra and inter-orbitals correlations are present while on Fe sites intervene only interactions between the same spin direction on different orbitals. Site energies are calculated using a mean-field approximation,

$$\tilde{E}_{\text{Fe}} = E_{\text{Fe}} + \frac{2}{3} U_{\text{eff}}^{\text{Fe}} \langle n_{\alpha\downarrow}^{\text{Fe}} \rangle, \quad (9)$$

$$\tilde{E}'_{\text{Fe}} = E'_{\text{Fe}} + \frac{2}{3} U_{\text{eff}}^{\text{Fe}} \langle n_{\beta\uparrow}^{\text{Fe}} \rangle, \quad (10)$$

$$\tilde{E}_{\text{Mo},\sigma} = E_{\text{Mo}} + \left(U^{\text{Mo}} + \frac{2}{3} J^{\text{Mo}} \right) \langle n_{\beta,-\sigma}^{\text{Mo}} \rangle + \frac{2}{3} U_{\text{eff}}^{\text{Mo}} \langle n_{\beta,\sigma}^{\text{Mo}} \rangle \quad (11)$$

and

$$\tilde{E}'_{\text{Mo},\sigma} = E'_{\text{Mo}} + \left(U^{\text{Mo}} + \frac{2}{3} J^{\text{Mo}} \right) \langle n_{\alpha,-\sigma}^{\text{Mo}} \rangle + \frac{2}{3} U_{\text{eff}}^{\text{Mo}} \langle n_{\alpha,\sigma}^{\text{Mo}} \rangle, \quad (12)$$

where $U_{\text{eff}}^{\text{Fe}} = U^{\text{Fe}} - J^{\text{Fe}}$, $U_{\text{eff}}^{\text{Mo}} = U^{\text{Mo}} - J^{\text{Mo}}$ and we used that $\langle n_{i\nu\sigma} \rangle = \langle n_{i\sigma} \rangle / 3$ due to the degeneracy of the three t_{2g} orbitals. $U_{\text{eff}}^{\text{Fe}} = 3w$, $U_{\text{eff}}^{\text{Mo}} = w$ and $J^{\text{Mo}} = 0.1w$ provide a good agreement with experimental data in disordered samples for $x = 0$ [13], so we take these values in the following calculations. The effective charge transfer energy, which determines the density of states and electronic properties, is related self-consistently with correlations and disorder. We shall take as a reference the charge transfer energy in the ideal case ($a = 1$ and $x = 0$),

$$\Delta = \tilde{E}_{\text{Mo},\downarrow}^o - \tilde{E}_{\text{Fe}}^o = E_{\text{Mo}} - E_{\text{Fe}} + \frac{2}{3} U_{\text{eff}}^{\text{Mo}} \langle n_{\beta,\downarrow}^{\text{Mo}} \rangle^0 - \frac{2}{3} U_{\text{eff}}^{\text{Fe}} \langle n_{\alpha,\downarrow}^{\text{Fe}} \rangle^0,$$

all the superscripts 0 allude to this state. This fixes the bare charge transfer energy $\Delta_0 = E_{\text{Mo}} - E_{\text{Fe}}$. It has been shown that this energy should be quite small [3], to reproduce the mixed-valence character $\zeta \sim 0.5$ observed experimentally [22,23].

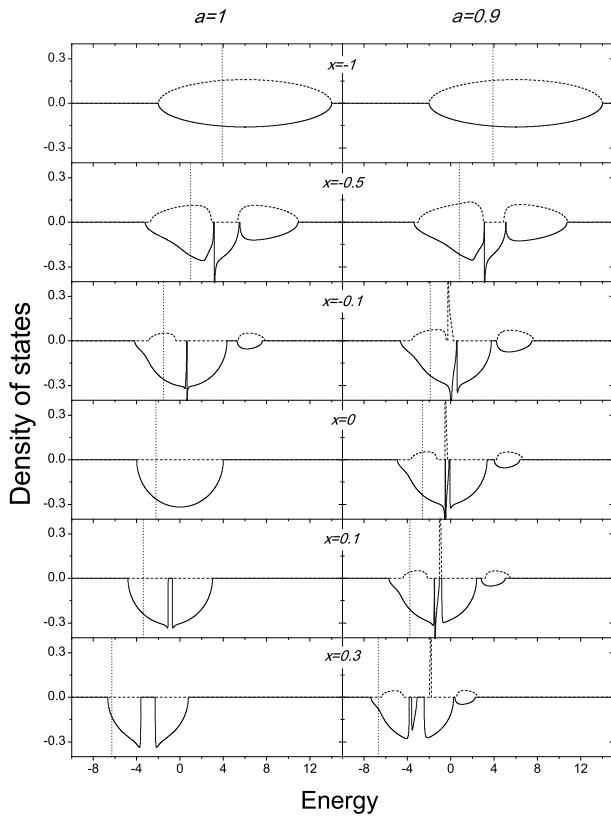


Fig. 2. Evolution of the density of states as a function of the composition x with $a = 1$ and $a = 0.9$ ($q = 2$). Solid (dotted) lines correspond to the spin down (up) channel. Dashed lines indicate the Fermi energy.

3 Results and discussion

In Figure 2 we show our results for the density of states over the whole range $-1 \leq x \leq 1/3$ taking $q = 2$. The paramagnetic metallic behavior and the Mo valency $4+$ is correctly reproduced for SrMoO_3 ($x = -1$). Let us first examine the off-stoichiometric system without disorder ($a = 1$). Note that our results correspond only to the description of the higher energy part of the t_{2g} bands, around and above the Fermi energy obtained in the band structure calculation [14]. We see that our DOS are qualitatively in good agreement with those of Zhu et al. In the Fe-rich regime ($x \geq 0$), spin up electrons cannot move because all α -sites are occupied by Fe \uparrow . So, the ground state remains half-metallic for $x > 0$ and the itinerant moment $M_i = 1 - 3x$ as shown in Figure 3a. The spin-up band above the Fermi level seen in the DOS of Zhu et al. corresponds to next n.n. (n.n.n) Mo–Mo hopping within sublattice β which, in our case, appears as a level at $\tilde{E}_{\text{Mo},\uparrow}$ since n.n.n hoppings are not included in our calculation. An effective charge transfer energy increases with increasing x due to the renormalization of the levels reaching Δ_0 as $x \rightarrow 1/3$. At the same time the down-spin band width is slightly reduced as a result of the increasing number of Fe \downarrow on the β -sublattice restricting the movement of down-spin electrons. The behavior in the $x \leq 0$ region is quite different, showing the appearance of

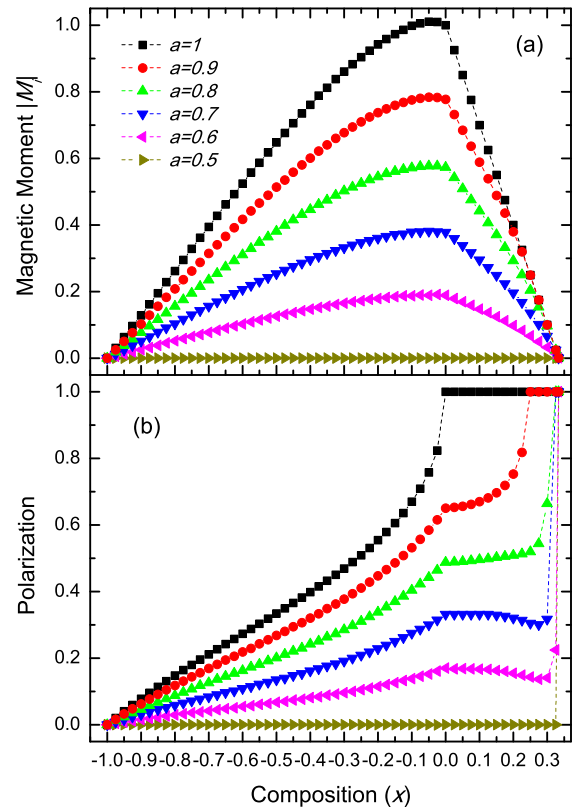


Fig. 3. (Color online) (a) Itinerant magnetic moment and (b) spin polarization over the whole range $-1 \leq x \leq 1/3$ with $q = 2$ for several values of the order parameter a .

up-spin states resulting from Mo–Mo hopping only forming a bonding band at the Fermi level. There is an important difference between our results and those of Zhu et al. In the results of Zhu et al. the lower bonding part is almost entirely below the Fermi level, therefore this should give an unrealistic valence lower than $4+$ of the Mo (AS), as discussed in the limit of low concentration of Mo (AS) ($x \rightarrow 0$) [13]. We suspect that this is a consequence of neglecting correlations on Mo sites. In our case, Mo correlations pushes the effective levels towards higher energies reducing the electron occupation at these Mo (AS) to realistic values. This affects both the itinerant magnetic moment $M_i = \langle n_\uparrow \rangle - \langle n_\downarrow \rangle$ and the spin polarization $P = \frac{D_\uparrow - D_\downarrow}{D_\uparrow + D_\downarrow}$, D_\uparrow and D_\downarrow being the DOS at the Fermi energy for up and down spin electrons, as shown in Figures 3a, 3b.

With disorder, in the $x \geq 0$ case the situation changes drastically: Mo (AS) starts to appear and the DOS resembles qualitatively the ordered $x \leq 0$ case, the system loosing its half-metallic character. However, the up spin Mo states at the Fermi level are now hybridized with the Fe (AS) states as the Mo are with Fe (S) in the down spin channel. In the $x \leq 0$ regime, no qualitative changes are expected since Mo (AS) were already present in the ordered case, the existence of Fe (AS) just modifies quantitatively the results. Of course, the M_i and P are reduced by the disorder, Figures 4a, 4b, and $M_i = 0$ in the fully

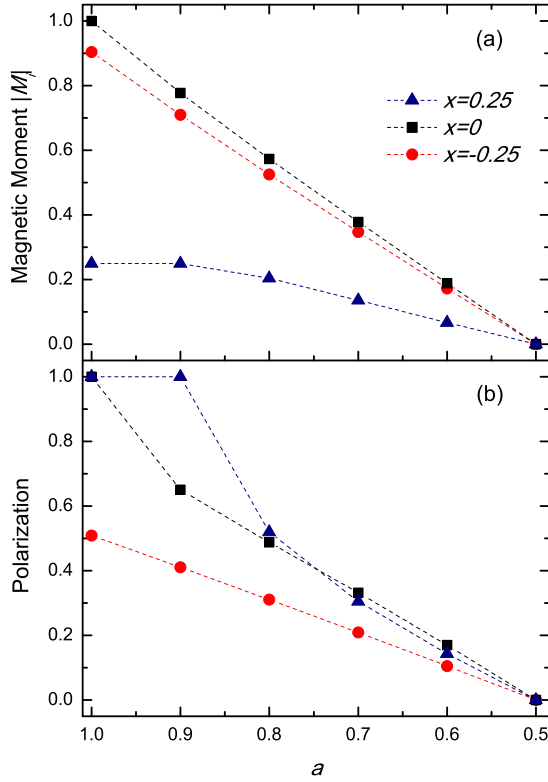


Fig. 4. (Color online) Behavior of (a) itinerant magnetic moment and (b) spin polarization as a function of a with $q = 2$ for both stoichiometric and off-stoichiometric systems.

disordered system ($a = 0.5$) because of the $\alpha - \beta$, $\uparrow - \downarrow$ symmetry in that case.

Of course, we cannot avoid a more detailed comparison with the experimental results of Topwal et al. [11]. M_S has two contributions: namely the one (M_{Fe}) from localized moments of Fe and the one (M_i) from the itinerant electrons. For the local moment contribution, $M_{Fe} = 5(p_{Fe}^\alpha - p_{Fe}^\beta)$ we get $M_{Fe} = 5(2a - 1)(1 + x)$ and $M_{Fe} = 5(2a - 1)(1 - x)$ respectively for $x \leq 0$ and $x \geq 0$. This is the main contribution to the total magnetization since $-1 \leq M_i \leq 0$. We see that M_i remains always opposite to the local magnetization M_{Fe} and $|M_i|$ follows qualitatively the same trend as M_{Fe} and the experimental M_S as function of x . In Figure 5, we show M_i and $M_S = M_{Fe} + M_i$ calculated for the reported values of the degree of order, a , in the different samples studied by Topwal et al. [11] i.e. 0.65, 0.83, 0.92, 0.89, 0.91, 0.90, 0.86 and 0.83 for $x = -0.5, -0.25, -0.1, -0.05, 0, 0.05, 0.1$ and 0.25 respectively. Our calculated values of M_S compare remarkably well with the measured ones using $q = 2$ and the agreement is even improved considering a slightly smaller Mo–Mo bandwidth $w'(q = 1.6)$.

Finally, it is also interesting to comment on the itinerant moment $\mu_\beta^{Mo} = \langle n_{\beta,\uparrow}^{Mo} \rangle - \langle n_{\beta,\downarrow}^{Mo} \rangle$ at Mo(S) and $\mu_\alpha^{Mo} = \langle n_{\alpha,\uparrow}^{Mo} \rangle - \langle n_{\alpha,\downarrow}^{Mo} \rangle$ at Mo(AS) shown in Figures 6a and 6b respectively. In the whole range of concentration the moment at Mo(S) shows a similar trend as the total itinerant moment. It is always opposite to the Fe local

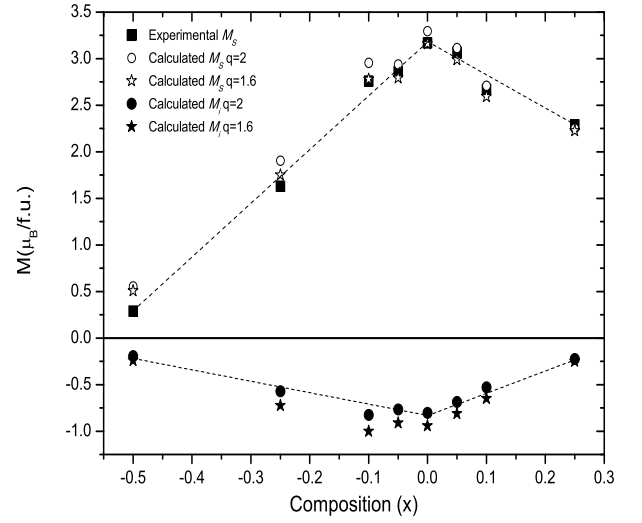


Fig. 5. Comparison of calculated and experimental saturation magnetic moment. Contribution of itinerant electrons is also shown.

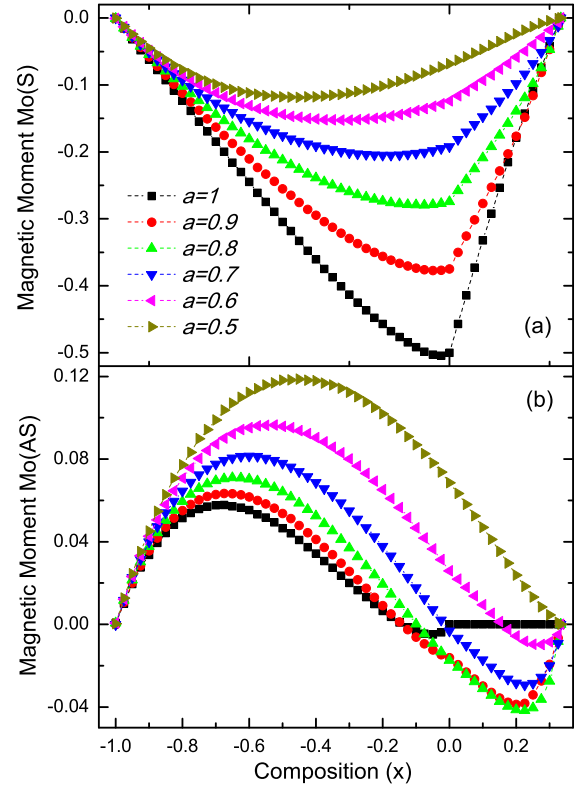


Fig. 6. (Color online) Itinerant magnetic moment for all compositions in (a) sites and (b) antisites positions with and without disorder.

moment on the correct α site, its amplitude remains quite large in a wide range of order and composition, varying between 0, (for $x = -1$ and $x = 1/3$) and -0.5 (for $x = 0$ and $a = 1$). It is reduced by the disorder. On the other hand, on the AS the moment is rather small, always $\lesssim 0.12$. The precise value of the moment depends critically on the position of the \uparrow -spin states due to the renormalization of

the Mo-level. Accordingly, the precise value and, of course, the sign of μ_{α}^{Mo} should not be taken too seriously, the only point that we should remember is that it is small. Of course, for $a = 0.5$, the moments on Mo(S) and Mo(AS) are just opposite, μ_{α}^{Mo} being positive and negative μ_{β}^{Mo} , consistent with $M_i = 0$. Basically, the magnetic picture is quite simple: Fe(S)–Mo(S) electron hopping keep the moment on Mo sites antiparallel to the local moment on Fe sites as in the stoichiometric case, while on Mo antisites the moment results from the strong Mo(AS) character of the \uparrow -channel bonding states below the Fermi energy giving an important contribution to $\langle n_{\alpha,\uparrow}^{\text{Mo}} \rangle$ which may almost compensate the \downarrow -spin part.

In summary, our approach based on a strongly correlated description for Fe with localized spins $S = 5/2$ and $n = 1 - 3x$ itinerant electrons reproduces extremely well the experimental behavior of the magnetization in the $\text{Sr}_2\text{Fe}_{1+x}\text{Mo}_{1-x}\text{O}_6$ ($-1 \leq x \leq 1/3$) family [11], providing deep theoretical grounds for the understanding of these double-perovskite materials. At the same time, this shows that it is rather reasonable to consider the disorder as random. Our results also confirm clearly the importance of the Mo correlations, although moderate ~ 1 eV, in determining an appropriate electronic scheme in these systems, off-stoichiometric and/or disordered.

J.R.S. thanks CONACyT México for financial support (129905). M.A. is grateful to D.D. Sarma for stimulating discussions. F.E. and O.N. want to acknowledge partial support from CONACyT México and PAPIIT-IN108710 from UNAM.

References

1. T.K. Mandal, M. Greenblatt, in *Functional Oxides*, edited by D.W. Bruce, D. O'Hare, R.I. Walton (Wiley, 2010), pp. 257–293
2. K.I. Kobayashi, T. Kimura, H. Sawada, K. Terakura, Y. Tokura, *Nature* **395**, 677 (1998)
3. E. Carvajal, O. Navarro, R. Allub, M. Avignon, B. Alascio, *Eur. Phys. J. B* **48**, 179 (2005)
4. D.D. Sarma, P. Mahadevan, T. Saha-Dasgupta, S. Ray, A. Kumar, *Phys. Rev. Lett.* **85**, 2549 (2000)
5. Hua Wu, *Phys. Rev. B* **64**, 125126 (2001)
6. Y. Tomioka, T. Okuda, Y. Okimoto, R. Kumai, K.I. Kobayashi, Y. Tokura, *Phys. Rev. B* **61**, 422 (2000)
7. S. Ray, A. Kumar, S. Majumdar, E.V. Sampathkumaran, D.D. Sarma, *J. Phys.: Condens. Matter* **13**, 607 (2001)
8. M. Bibes, F. Bouzehouane, A. Barthélémy, M. Besse, S. Fusil, M. Bowen, P. Seneor, J. Carrey, V. Cros, A. Vaurès, J.P. Contour, A. Fert, *Appl. Phys. Lett.* **83**, 2629 (2003)
9. D.D. Sarma, E.V. Sampathkumaran, S. Ray, R. Nagarajan, S. Majumdar, A. Kumar, G. Nalini, T.N. Guru Row, *Solid State Commun.* **114**, 465 (2001)
10. M. García-Hernández, J.L. Martínez, M.J. Martínez Lope, M.T. Casais, J.A. Alonso, *Phys. Rev. Lett.* **86**, 2443 (2001)
11. D. Topwal, D.D. Sarma, H. Kato, Y. Tokura, M. Avignon, *Phys. Rev. B* **73**, 94419 (2006)
12. T. Saha-Dasgupta, D.D. Sarma, *Phys. Rev. B* **64**, 064408 (2001)
13. B. Aguilar, O. Navarro, M. Avignon, *Europhys. Lett.* **88**, 67003 (2009)
14. X.F. Zhu, Q.F. Li, L.F. Chen, *J. Phys.: Condens. Matter* **20**, 075218 (2008)
15. J. Linden, M. Karppinen, T. Shimada, Y. Yasukawa, H. Yamauchi, *Phys. Rev. B* **68**, 174415 (2003)
16. C. Meneghini, S. Ray, F. Liscio, F. Bardelli, S. Mobilio, D.D. Sarma, *Phys. Rev. Lett.* **103**, 046403 (2009)
17. P. Mahadevan, N. Shanti, D.D. Sarma, *J. Phys.: Condens. Matter* **9**, 3129 (1997)
18. R. Agarwal, Z. Singh, V. Venugopal, *J. Alloys Compds.* **282**, 231 (1999)
19. E.N. Economou, *Green's Functions in Quantum Physics* (Springer, Berlin, 2006)
20. H. Shiba, *Prog. Theor. Phys.* **46**, 77 (1971)
21. Y.S. Lee, J.S. Lee, T.W. Noh, Douck Young Byun, Kwang Soo Yoo, K. Yamaura, E. Takayama-Muromachi, *Phys. Rev. B* **67**, 113101 (2003)
22. J. Lindén, T. Yamamoto, M. Karppinen, H. Yamauchi, T. Pietari, *Appl. Phys. Lett.* **76**, 2925 (2000)
23. O. Chmaissem, R. Kruk, B. Dabrowski, D.E. Brown, X. Xiong, S. Kolesnik, J.D. Jorgensen, C.W. Kimball, *Phys. Rev. B* **62**, 14197 (2000)